

Titania–Silica Mixed Oxides

II. Catalytic Behaviour in Olefin Epoxidation

R. Hutter, T. Mallat, and A. Baiker¹

Department of Chemical Engineering and Industrial Chemistry, Swiss Federal Institute of Technology,
ETH-Zentrum, CH-8092 Zurich, Switzerland

Received September 23, 1994; revised December 1, 1994

Various titania–silica aerogels prepared by an alkoxide-sol-gel route have been tested in the epoxidation of bulky olefins using cumene hydroperoxide as oxidant. The drying method, the titanium content between 2 and 20 wt%, and the calcination temperature between 473 and 1073 K were the most important preparation parameters, influencing the catalytic behaviour of the aerogels. The aerogels dried by semicontinuous extraction with supercritical CO₂ at low temperature (LT aerogel) were found to be much more efficient epoxidation catalysts than aerogels prepared by high-temperature supercritical drying and conventionally dried xerogels. The reaction rate of cyclohexene epoxidation over LT aerogels increased monotonically with increasing Ti content. In the range of 333–363 K the catalysts containing 20 wt% TiO₂ (20LT) showed high activity and selectivity (79–93% to peroxide and 87–100% to epoxide) in the oxidation of various cyclic olefins, including cyclododecene, norbornene, cyclohexene, and limonene. Catalytic experiments, FTIR, and UV–vis spectroscopy indicated that the LT aerogels consist of two different types of active species: titanium well-dispersed in the silica matrix and titania nanodomains. The key factors determining the activity and selectivity of sol-gel titania–silica catalysts are the morphology (surface area and pore size) and the relative proportions of Ti–O–Si and Ti–O–Ti structural parts. A comparative study of the epoxidation of cyclohexene, cyclododecene, and norbornene over structurally different titania–silica catalysts, indicates that 20LT shows better catalytic behaviour in these reactions than Ti zeolites and silica-supported titania. © 1995 Academic Press, Inc.

INTRODUCTION

The epoxidation of olefins has attracted considerable interest due to the versatility of epoxides as intermediates in organic synthesis (1). Various oxides and supported oxides have been proposed for substituting homogeneous transition metal catalyzed epoxidations, but their activity was found to be due to rapid dissolution of the surface

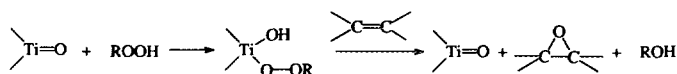
layer and the *in situ* formation of a homogeneous catalyst (2). A silica-supported titania was the first active and really heterogeneous catalyst discovered in the early 1970s (3, 4). The catalyst contains ca. 2 wt% TiO₂, prepared by the reaction of a Ti compound with high surface area silica. Its activity is likely due to the development of isolated surface titanyl groups during calcination. The active species are surface Ti–alkylperoxy groups, which are formed by the reaction with alkylhydroperoxides (2, 5), according to Scheme 1.

The crucial role of Ti^{IV} isolated by O–Si^{IV} fragments is demonstrated by the much lower activity of titania supported on other oxides or that of the physical mixture of titania and silica (2, 5). After silylation, which removes the Brønsted acidity of the residual surface Si–OH groups, the Shell catalyst provides 91–95% selectivity towards propylene oxide at 96–97% peroxide conversion.

The discovery of titanium-substituted zeolites with MFI (TS-1) and MEL (TS-2) structures opened a new direction in the development of heterogeneous oxidation catalysts (6, 7). In titanium silicalites titanium is uniformly distributed in the crystalline framework by isomorphous substitution of a part of Si^{IV} with Ti^{IV} (8). These materials are active at near ambient temperature and catalyze a variety of reactions with H₂O₂ as oxidant, including the epoxidation of olefins (5, 9, 10). After addition of H₂O₂ the catalyst turns yellow, which is attributed to the reversible formation of a surface Ti–peroxy compound (I) or that of the dissociated form (II) at high pH (11) (Scheme 2). Silylation of titanium silicalite is efficient in suppressing the hydration of epoxide to glycol and 98% epoxide selectivity at 92% H₂O₂ conversion has been reported in propylene oxidation (5).

The application of titanium silicalite is limited to relatively small reactants which are able to penetrate into the narrow channels of 0.55 nm average size where most of the active sites are situated. This limitation is well demonstrated by the observation that 1-hexene is oxidized

¹ To whom correspondence should be addressed.



SCHEME 1

about hundred times faster than cyclohexene (11). A considerable effort has been expended in the past years to overcome this restriction by synthesizing large- and ultralarge-pore titanium-containing zeolites isomorphous to zeolite β (12) or MCM-41 (13). For bulky reactants they are superior to titanium silicalite, as expected from the steric limitations in the latter, but their intrinsic oxidation activity for C_6 – C_{12} aliphatic alkenes is lower than that of titanium silicalite (14). Moreover, the yields are remarkably lower than those in TS-1 catalyzed reactions. In the oxidation of C_6 – C_{12} cycloolefins the selectivities are only 70 to 90% even at moderate (30–80%) H_2O_2 conversion (13, 14). In the oxidations of higher alkenes, complications arise due to the immiscibility of the reactant and the aqueous H_2O_2 solution (15).

A further possibility for synthesizing Ti- and Si-containing catalysts with interactions between the two components at the atomic level is the application of the solution-sol-gel technique (16–19). The first attempts to use sol-gel-derived titania–silica xerogels for the liquid-phase epoxidation of olefins were reported recently by Neumann *et al.* (20). The authors found that only traces of epoxide formed over sol-gel titania–silica in 20 h during the oxidation of cyclohexene or cyclooctene, even when they used an equimolar amount of H_2O_2 at 333 K. In another study (21) the activity of titania–silica mixed oxides was somewhat higher when a non-aqueous alkylhydroperoxide was used as oxidant.

In order to explore the potential of sol-gel-derived titania–silica aerogels as epoxidation catalysts, we have first studied systematically the influence of the sol-gel and drying conditions on the structural and chemical properties of these materials (22) (part I of this work). It has been demonstrated that amorphous, high surface area titania–silica aerogels with excellent titanium dispersion up to 20 wt% TiO_2 can be prepared using suitable preparation and drying conditions. The focus of this paper is on the catalytic properties of these materials in the epoxidation

of olefins. It is demonstrated that the proper selection of the preparation conditions results in excellent oxidation catalysts.

EXPERIMENTAL

Catalyst Preparation

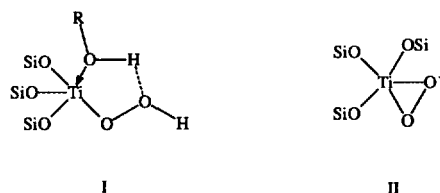
Aerosil 200 (Degussa, $S_{BET} = 200 \text{ m}^2/\text{g}$) was used as an amorphous silica, and P25 (Degussa, $S_{BET} = 50 \text{ m}^2/\text{g}$) made up of 70% anatase and 30% rutile was used as a crystalline titania sample. Amorphous titania ($S_{BET} = 288 \text{ m}^2/\text{g}$) was prepared by the sol-gel-aerogel method using titanium-*n*-butoxide (ALFA) as precursor and dried by semicontinuous extraction with supercritical CO_2 (low-temperature aerogel) (23). Titanium silicalite (TS-1; 3.1 wt% TiO_2 , $S_{BET} = 420 \text{ m}^2/\text{g}$) has been synthesized based on the recipe described in Ref. (24). Ion-exchanged and doubly distilled water was used for the preparations.

Detailed information on the synthesis and characterization of sol-gel titania–silica has been given in part I (22). The same acronyms for the samples are used in the present paper and reported herein for convenience. 10LTp is presented as an example: The numbers before the letters denote the Ti content expressed as TiO_2 in weight percent. The subsequent two capital letters represent the drying method used (low-temperature supercritical drying \rightarrow LT; high-temperature supercritical drying \rightarrow HT; xerogel \rightarrow X). The letter p at the end indicates the prehydrolysis of the Si compound before addition of the Ti compound.

All sol-gel titania–silica catalysts were synthesized under acidic preparation conditions. The resulting gels were dried by three different methods: (i) conventional drying (xerogels), (ii) high-temperature supercritical drying (HT aerogels), and (iii) semicontinuous extraction with supercritical CO_2 (LT aerogels). In a typical synthesis, an acidic hydrolysant was added to an isopropanolic solution of tetraisopropoxytitanium(IV) (TIPOT) modified by acetylacetone (acac) (molar ratio TIPOT:acac = 1:1) and tetramethoxysilicon(IV) (prehydrolyzed or not). The resulting titania–silica gels were subsequently dried and calcined in air. The maximum temperature applied was 373 K in conventional drying, 533 K in high-temperature drying, and 313 K in low-temperature drying.

The basis of preparation of the silica-supported titania catalysts (titania-on-silica) is a patent to Shell (4). The suggested process was modified by using (i) a specially pretreated support and (ii) grafting, instead of incipient wetness for the immobilization of titanium.

The carrier was pretreated as follows: Aerosil 200 was hydrated with water at 298 K for 90 min. Then water was removed in vacuum at 350 K. The dry aerosil was powdered and sieved. The fraction between 0.3–0.7 mm was heated to 473 K under an argon stream for 6 h and all further operations were performed under dry condi-



SCHEME 2

tions, in Ar. 10.0 g of pretreated silica was suspended in 10 ml *i*-PrOH, the freshly prepared grafting solution was added, and the suspension was refluxed for 18 h. The grafting solution contained TIPOT/acac/*i*-PrOH in a molar ratio of 1/2/35.

After filtration the residue was washed with *i*-PrOH and dried at 353 K under vacuum (1 Pa) for 1 h. The calcination procedure was performed in a tubular reactor and involved a heating step in a nitrogen stream (50 ml min⁻¹) up to 573 K at a rate of 5 K min⁻¹. After 1 h treatment at the maximum temperature the sample was cooled rapidly to 353 K. The next step was a heat treatment in dry air (400 ml min⁻¹). The temperature was ramped at a rate of 5 K min⁻¹ up to 873 K, held at this value for 4 h, and then decreased rapidly to 353 K.

The Ti content of the samples was determined by inductively coupled plasma atomic emission spectroscopy (ICP-AES). The catalyst samples were stored in closed vessels in air.

Physicochemical Methods

All spectroscopic measurements were made at room temperature. Infrared analysis of the samples was performed on a Perkin-Elmer 2000 FTIR. 100 scans were accumulated for each spectrum at a spectral resolution of 4 cm⁻¹. One milligram sample in 100 mg dry KBr was compressed to a wafer and placed directly into the IR beam. For the study of the interaction of Ti^{IV} with the oxidant, 20 mg catalyst was wetted with 2 ml H₂O₂ (35% in water), stirred for 5 min at room temperature, filtered, and freeze dried.

A Perkin-Elmer Lambda 16 spectrophotometer equipped with a 76-mm integrating sphere using BaSO₄ as reference was used to record the UV-vis diffuse reflectance spectra of the powder samples under ambient conditions. A special quartz sample cell was constructed to allow *in situ* characterization of the samples. The samples were heated to 473 K under an argon flow for 5 h and cooled to room temperature before the spectrum was recorded. The Kubelka-Munk function (25) was used to show the experimental data. Impregnation of the samples with H₂O₂ was performed as described above.

Epoxidation Procedure

Cumene hydroperoxide (pract.; 80 wt% in cumene), H₂O₂ (35 wt% in H₂O; purum), and methanol (puriss. p.a.) (all from Fluka) were used as received. Cumene (purum), 2-phenyl-2-propanol (purum), toluene (purum), cyclohexene (purum), cyclohexene oxide (purum), 1-hexene (purum), 1-hexene oxide (purum), cyclododecene (*cis* + *trans*; pract.), cyclododecene oxide (*cis* + *trans*; pract.), (±)-limonene (purum) (all purchased from Fluka), norbornene (99%), 2,3-epoxynorbornane (98%), and (±)-limo-

nene oxide (97%) (all from Aldrich) were purified by distillation prior to use. Sodium iodide (puriss. p.a.), acetic acid (puriss. p.a.), isopropylalcohol (puriss.; absolute), and sodium thiosulfate 0.1 N standard solution, for iodometric titration, were used as received.

The catalytic runs were carried out batchwise in a mechanically stirred, closed 100-ml glass reactor fitted with reflux condenser, thermometer, septum for withdrawing samples, and dropping funnel for addition of the peroxide. The reaction temperature was maintained constant within ±0.5 K using a thermostated bath. All reactions were performed strictly under argon (99.999%) to avoid the presence of oxygen and moisture. In a typical run, air was removed from the system by means of an argon flow and a vacuum pump prior to reaction. An amount of 16.7 ml (13.4 mmol) of 12 wt% cumene hydroperoxide (CHP) in cumene was charged in the dropping funnel. Then 100 mg catalyst and 7.8 ml (77 mmol) cyclohexene were introduced into the reactor. The solutions were heated to reaction temperature (usually 333 K) and the reaction was started by adding the peroxide to the vigorously stirred slurry. These standard conditions were used if not otherwise stated.

The conditions of the catalytic runs using H₂O₂ as oxidant were as follows: olefin, 0.9 M; H₂O₂, 0.18 M; catalyst, 5 g/liter; solvent, methanol; temperature, 363 K.

Aliquots were removed at various time intervals, filtered, and analyzed by gas chromatography (HP 5890 equipped with an autosampler, a flame ionization detector, and a capillary column HP-1). A cool on-column inlet for automatic injection was used to avoid undesired reactions in the injection port. The injection temperature was 313 K, lower than the reaction temperature. Concentrations were calculated based on peak areas, and at the end of the reaction an internal standard (toluene) was added to the slurry in order to check if there was any loss of product. The initial rate was defined as the epoxide formation in the first 300 s. Hydroperoxide conversion was determined by iodometric titration (26) using a Metrohm 686 Titroprocessor.

The selectivities (*S*) obtained in the epoxidation experiments are calculated in the following way:

$$S_{\text{peroxide}} (\%) = 100 \cdot [\text{epoxide}]_f / ([\text{peroxide}]_i - [\text{peroxide}]_f)$$

$$S_{\text{olefin}} (\%) = 100 \cdot [\text{epoxide}]_f / ([\text{olefin}]_i - [\text{olefin}]_f)$$

All concentrations are expressed on a molar basis. The subscripts *i* and *f* stand for initial and final values, respectively.

For the determination of the experimental error, the epoxidation reaction was repeated four times with 10LT calcined at 873 K. The calculated standard deviation was ca. ±2% for initial rates, ca. ±1% for conversion after 90 min, and ca. ±2% for *S*_{peroxide}.

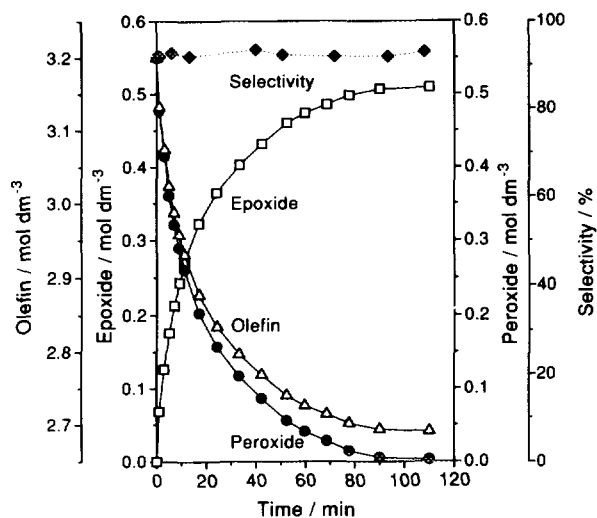


FIG. 1. Concentration of peroxide (●), olefin (Δ), and epoxide (□), and peroxide selectivity (S_{peroxide}) (◆) during the epoxidation of cyclohexene with CHP at 333 K over 20LT aerogel calcined at 873 K.

The minimum energy conformation of CHP and the olefins was calculated by MM+ force field (Hyperchem, Release 3 from Hypercube, Inc.).

RESULTS

General Features of the Epoxidation Reaction

Figure 1 shows the epoxidation of cyclohexene with CHP using the 20LT aerogel catalyst, which proved to be the best in this reaction. Under these conditions the reaction is fast and selective. After 70 min 95% of the peroxide is consumed, with 93% selectivity (S_{peroxide}) to cyclohexene oxide. S_{peroxide} was independent of conversion. The decomposition of the alkylhydroperoxide to oxygen was negligibly small. Note that metal catalyzed epoxidations are often accompanied by radical decomposition of the peroxide reagent, forming oxygen and a variety of organic by-products (27). The decomposition of CHP over various catalysts, in the absence of an olefin, will be discussed later. The selectivity based on the olefin (S_{olefin}) was ca. 100%. No by-product formation derived from cyclohexene was detected with GC. Tar formation could be excluded by using an internal standard.

Influence of Drying Method

Three titania-silica catalysts, containing 10 wt% TiO₂ and prepared the same way but dried with different methods, are compared in Fig. 2. The LT aerogel (10LT) shows an outstanding activity compared to the HT aerogel (10HT), and the xerogel (10X) is practically inactive. This trend has been observed for all sol-gel titania-silica cata-

lyst series, independent of the calcination temperature, Ti content, or chemical nature of the reactant (1-hexene, cyclohexene, or limonene). Accordingly, the overall tendency in the epoxidation activity of sol-gel catalysts is as follows: LT aerogels > HT aerogels > xerogels.

The structural and catalytic properties of some typical aero- and xerogels are compared in Table 1. The LT aerogels show the highest activity and selectivity for epoxide formation. The selectivity of HT aerogels is almost as good as that of LT aerogels. All xerogels induce some peroxide decomposition with a negligible selectivity for epoxide formation. Using uncalcined instead of calcined xerogel samples or 1-hexene (a smaller olefin which is readily oxidized by TS-1) instead of cyclohexene as reactant, the xerogels did not show higher oxidizing activity. Note that in our system not the olefin but the oxidant cumene hydroperoxide is the bulkiest molecule (calculated size in minimum energy conformation: $0.55 \times 0.63 \times 0.93$ nm).

Some of the important structural characteristics are also collected in Table 1. (More details can be found in part I (22).) All xerogels prepared by acidic hydrolysis and conventional drying exhibit a pronounced microporosity, whereas the aerogels are dominantly mesoporous. It seems that the low activity of xerogels is connected to limited accessibility in the very compact, glass-like material. N₂-physisorption data from microporous materials or high surface area aerogels have to be interpreted with caution (28). Besides, the surface area accessible to the reactants during reaction may be different from the BET areas due to solvation effects in liquid phase. A qualitative comparison of 10X, 10HT, and 10LT catalysts shows that

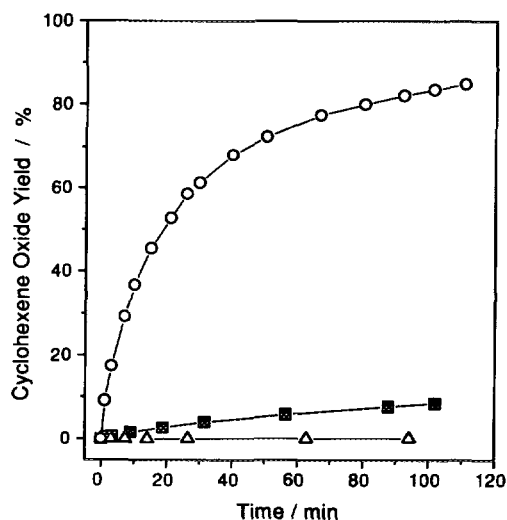


FIG. 2. Epoxidation of cyclohexene at 333 K with catalysts prepared by various drying methods and calcined at 873 K; 10LT aerogel (○), 10HT aerogel (■), and 10X xerogel (Δ).

TABLE 1
Catalytic Epoxidation of Cyclohexene with Cumene Hydroperoxide (CHP) at 333 K

| Sample ^a | $S_{\text{BET}}(S_t)^b$ ($\text{m}^2 \text{g}^{-1}$) | $V_p(\text{N}_2)^c$ ($\text{cm}^3 \text{g}^{-1}$) | $S_{\text{Si-O-Ti}}/S_{\text{Si-O-Si}}^d$ | $D_{\text{Si-O-Ti}}^e$ | Initial rate ($\text{mmol min}^{-1} (\text{g cat})^{-1}$) | Reaction time (h) | CHP conversion (%) | Selectivity (%) | |
|---------------------|---|--|---|------------------------|--|----------------------|--------------------------|-----------------------|---------------------|
| | | | | | | | | S_{peroxide} | S_{olefin} |
| 10X | 473(407) | 0.026 | 0.57 ^e | 6.8 ^f | 2.5×10^{-4} ^g | 18 | 10 | 2 | 88 |
| 10Xp | 399(337) | 0.020 | 0.59 ^e | 7.1 ^f | 2.2×10^{-4} ^g | 18 | 9 | 2 | 85 |
| 5HT | 553(1.4) | 2.7 | 0.12 | 3.0 | 0.15 | 2 | 9 | 85 | 95 |
| 10HT | 598(0) | 3.6 | 0.14 | 1.7 | 0.21 | 2 | 13 | 83 | 96 |
| 5LT | 518(208) | 0.99 | 0.38 | 9.5 | 2.95 | 2 | 74 | 92 | 100 |
| 10LT | 683(140) | 1.7 | 0.49 | 5.9 | 6.01 | 2 | 94 | 92 | 100 |

Note. Designations of the samples are explained under Experimental.

^a All samples have been calcined at 673 K prior to use.

^b (S_t), in parentheses, denotes specific micropore surface area derived from t -plot analysis.

^c Pore volume of pores in the maximum range 1.7 and 300 nm diameter.

^d Relative contribution of Si-O-Ti entities estimated from the ratio of the peak areas for Si-O-Ti (930–939 cm^{-1}) and Si-O-Si (1205–1215 cm^{-1}) determined by deconvolution of the original FTIR spectra.

^e Estimate of Ti dispersion derived from Eq. [1] in Ref. (22).

^f Spectra of the raw samples.

^g Initial rate was determined after 1 h instead of 300 s.

the surface areas are comparable (within a range of $\pm 20\%$), but the pore volume (pores in the maximum range 1.7 and 300 nm diameter) of the low-activity 10X sample is 65–140 times smaller than that of the aerogels.

Effect of Calcination Temperature

The influence of calcination temperature on the catalytic behaviour and properties of the aerogels, influenced by the calcination, is illustrated in Fig. 3, using the 10LT aerogel as an example. Calcination in air up to 673 K increased the (free) surface area, due to the oxidative removal of the organic residues (22). Interestingly, the highest activity was measured on the raw sample, and the substantial loss of surface area between 673 and 1073 K calcination temperatures (ca. 33%) is not reflected in the epoxidation activity. It seems that the organic residues originating from catalyst preparation favour the epoxidation reaction. The phenomenon, that the raw sample exhibits the highest activity for epoxidation within a calcination series, has been observed for all investigated LT titania-silica aerogels. Besides, the calcination temperature has no significant influence on the epoxidation selectivity.

Influence of Ti Content and Prehydrolysis

The correlation between the catalytic performance of LT aerogels and their Ti content is shown in Fig. 4 and Table 2. For both types of catalysts (LT and LTp) the initial rate increases monotonically with titanium content.

The 20LT aerogel represents the most active solid of these catalysts. The activity of LT and LTp catalysts of equal titanium content does not significantly differ in the case of the samples containing 5 and 20 wt% TiO_2 ; i.e., prehydrolysis of the silicon precursor has no significant influence on the epoxidation reaction. A similar conclusion can be drawn from the comparison of 10X and 10Xp catalysts

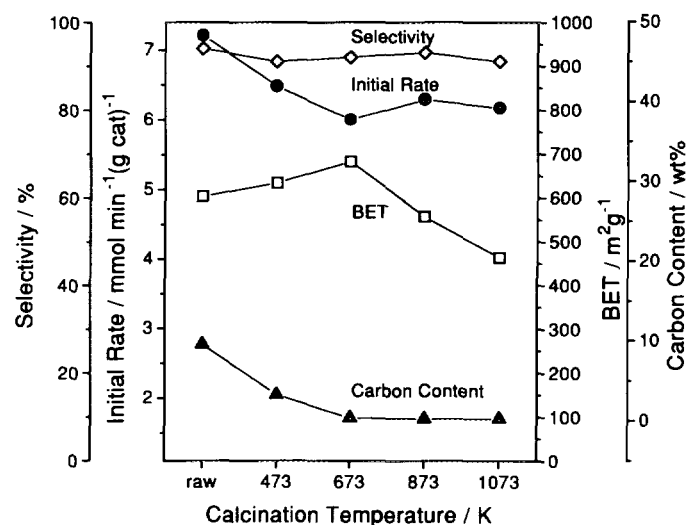


FIG. 3. Effect of calcination temperature on the carbon content of the samples (▲), the BET surface area (□), the selectivity (S_{peroxide}) (◇), and the initial rate (●) in cyclohexene epoxidation at 333 K over 10LT aerogel.

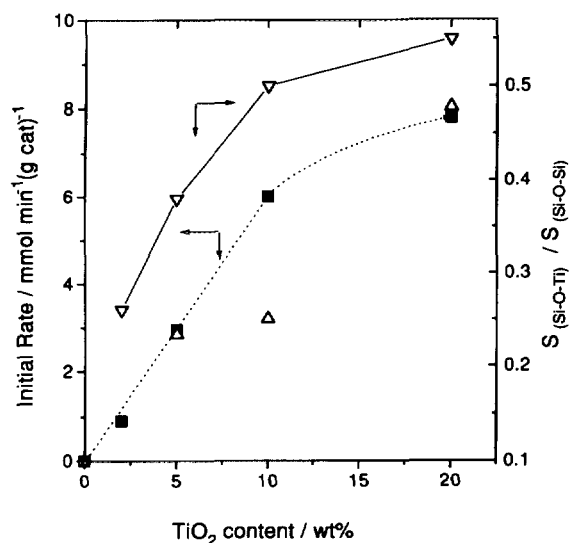


FIG. 4. Initial rate of cyclohexene epoxidation over LT (■) and LTp (△) aerogels as a function of Ti content and absolute contribution of Si–O–Ti connectivity of LT (▽) aerogel defined in part I (22). Rate is referred to weight of catalyst after calcination at 673 K.

(Table 1). The higher deviation between the activity of 10LT and 10LTp samples is likely due to some uncontrolled change during catalyst preparation.

Comparison of LT Aerogels, TS-1 and Titania-on-Silica

The catalytic performance of various titania–silica catalysts and component oxides in the oxidation of cyclohex-

ene with CHP is shown in Table 2. The order of the catalysts based on the epoxide yield (conversion times selectivity) in unit time is as follows: silica < titania (cryst.) < TS-1 < titania (amorphous) < titania-on-silica < LT aerogel.

The sol-gel titania–silica catalyst 20LT is compared to TS-1 in the epoxidation of cyclohexene (Fig. 5, Table 2). For this comparison the temperature was increased to 363 K. There is a striking difference in activity in favour of the sol-gel catalyst: the initial rate of epoxidation is 1.6×10^3 times higher on our catalyst than on TS-1. The low activity measured with TS-1 in oxidizing cyclohexene using CHP as oxidizing compound is a consequence of the limited accessibility of the active sites imposed by the zeolite micropore structure. The observed activity is likely due to the active sites located on the outer surface of the zeolite which are readily accessible also for bulky reactants. Also with H₂O₂, which is generally used as oxidant with TS-1 in a methanol/water solution (9), only negligible activity was measured in epoxidizing cyclohexene (<10% conversion after 24 h). This has been explained by restricted transition state shape selectivity and diffusivity effects of reagents and products (11). Using 1-hexene instead of cyclohexene, TS-1 showed a conversion of 65% in 2 h and a good selectivity ($S_{\text{peroxide}} = 88\%$) for the epoxidation in an aqueous/methanolic H₂O₂ solution at 313 K. This is an indication that our TS-1 sample is an acceptable reference material (14).

LT titania–silica aerogels and the titania-on-silica catalysts are the most effective for epoxidation with CHP

TABLE 2
Conversions and Selectivities of Various Catalysts in Cyclohexene Epoxidation at 333 K

| Catalyst | Calcination temp. (K) | Time (h) | CHP conversion (%) | Selectivity (%) | |
|---|-----------------------|----------|--------------------|-----------------------|---------------------|
| | | | | S_{peroxide} | S_{olefin} |
| SiO ₂ | 573 | 18 | 3 | 0 | 0 |
| TiO ₂ (P25) | 473 | 18 | 21 | 14 | 49 |
| TiO ₂ (amorphous) ^a | 623 | 20 | 37 | 63 | 69 |
| 5LT | 673 | 4 | 89 | 92 | 100 |
| 5LTp | 673 | 5 | 87 | 91 | 100 |
| 10LT | 673 | 1.5 | 84 | 92 | 100 |
| 10LTp | 673 | 1.5 | 63 | 90 | 100 |
| 20LT | 673 | 1.5 | 100 | 93 | 100 |
| 20LTp | 673 | 1.5 | 100 | 92 | 100 |
| 20LTp | — | 1.2 | 100 | 92 | 100 |
| TS-1 | 823 | 17 | 6 | 85 | 90 |
| 1 wt% TiO ₂ -on-SiO ₂ | 673 | 1.5 | 80 | 89 | 100 |
| 2 wt% TiO ₂ -on-SiO ₂ | 673 | 1.5 | 78 | 89 | 100 |

^a LT aerogel.

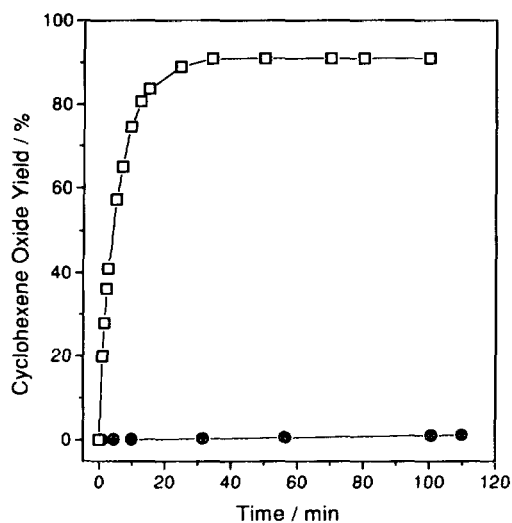


FIG. 5. Comparison of 20LT aerogel calcined at 873 K (\square) and TS-1 (\bullet) in the epoxidation of cyclohexene at 363 K.

(Table 2). The uncalcined 20LTp and 20LT aerogels show the highest oxygenation activity of all tested catalysts. An exact comparison of LT aerogels and titania-on-silica catalysts is difficult, as the Ti contents are different and the number of active sites is unknown. Usually titania-on-silica with an overall TiO_2 content of about 2 wt% is used for epoxidation (2–4). We attempted to prepare titania-on-silica with high (10–20 wt%) titania content, but the maximum loading that could be grafted under the applied conditions was 2.3 wt% according to ICP-AES analysis, and in agreement with earlier findings (29).

An interesting observation is the good activity and the unexpectedly high selectivity of sol-gel (amorphous) titania. This material has high BET surface area ($288 \text{ m}^2/\text{g}$) and small (primary) particle size (ca. 10 nm), which can explain—at least partly—the fact that its oxidation activity is higher than that of crystalline titania (P25, BET = $50 \text{ m}^2/\text{g}$). A similarly good activity but lower selectivity has been reported earlier (2) for bulk titania. The lower selectivity may be due to the higher temperature applied (383 K instead of 333 K). In epoxidations catalyzed by TS-1, TiO_2 (“extraframework” titanium) has activity only for H_2O_2 decomposition (30).

Spectroscopic Characterization

The FTIR spectra of three typical sol-gel titania-silica samples, containing 10 wt% TiO_2 and varying only in the drying method, are shown in Fig. 6b. The band at about 950 cm^{-1} is well-developed in both LT aerogel and xerogel, but only weak in the case of HT aerogel. This band is attributed to Si–O–Ti linkages (30–37) and indicates a good mixing of Ti and Si at the atomic level, as discussed in part I (22) of this work.

Figure 6a shows the changes in the IR characteristics of the samples occurring upon interaction with H_2O_2 . A treatment with H_2O_2 results in a decrease of the band at about 950 cm^{-1} in the IR spectra of LT aerogel (Fig. 6, top) and xerogel (Fig. 6, bottom). The intensity of the absorption can be related to that of the symmetric Si–O–Si-stretching vibration at ca. 800 cm^{-1} as an inner reference. The spectral changes are completely reversible: heating the samples at 333 K for 2 h restores the original IR spectra (Fig. 6b). The disappearance of this band upon interaction with H_2O_2 at room temperature and the appearance of a weak band at 880 cm^{-1} are attributed to the formation of solid Ti-peroxo complexes from the isolated Ti species (38). The weak band at 880 cm^{-1} is not observable in Fig. 6. Presumably it is covered by the broad band between 850 and 1000 cm^{-1} .

The characteristics of HT aerogels are different. There is no detectable change in the 950 cm^{-1} band after treat-

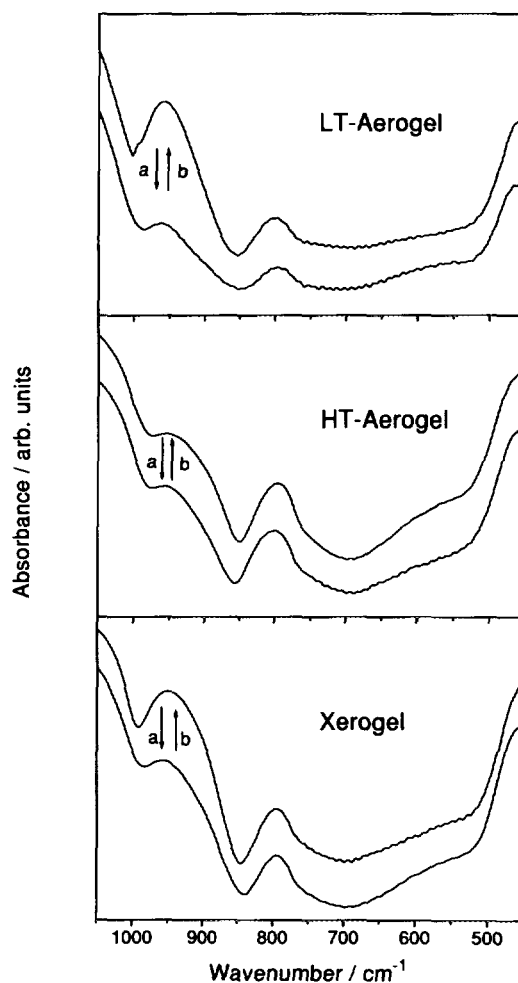


FIG. 6. FTIR spectra of 10LT aerogel (top), 10HT aerogel (middle), and 10X xerogel (bottom) after H_2O_2 adsorption (a) and after subsequent heating at 333 K (b).

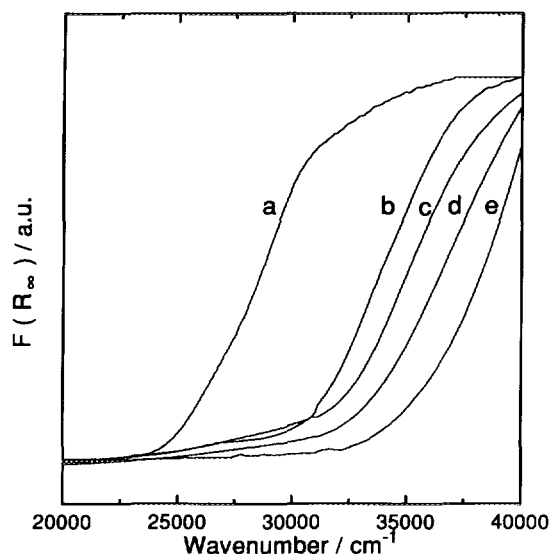


FIG. 7. Diffuse reflectance spectra of 10HT aerogel (a), 20LT aerogel (b), 10LT aerogel (c), 5LT aerogel (d), and TS-1 (e). The spectrum for anatase overlaps the spectrum for 10HT aerogel, so it is not shown.

ment with H_2O_2 (Fig. 6, middle). Note that the concentration of the Ti–O–Si species giving rise to the band at about 950 cm^{-1} is low in these materials due to the low Ti dispersion (22). This property makes the measurement of the changes induced by H_2O_2 difficult.

UV–vis spectroscopy is known to be a sensitive method for the characterization of titania–silica gels, titania-on-silica, and TS-1 (19, 30, 31, 35, 37, 39, 40). Spectra of some aerogels derived from UV reflectance data are presented in Fig. 7. The position of the UV absorption edge for 10HT aerogel sample (approximately at $28,000\text{ cm}^{-1}$) is almost the same as that for anatase (not shown). The absorption in the spectrum of TS-1 above $34,000\text{ cm}^{-1}$ is due to a charge transfer between Ti^{IV} and lattice oxygen in zeolitic Ti–O (31, 39). Charge transfer bands at lower wavenumbers typical for anatase and occluded TiO_2 (at ca. $30,500\text{ cm}^{-1}$) (30) are absent, which ensures that this TS-1 sample is well-manufactured.

The absorption edges of all LT aerogels are between those characteristic of anatase ($28,000\text{ cm}^{-1}$) and TS-1 ($34,000\text{ cm}^{-1}$). As the Ti content of the mixed oxides increases, the UV absorption edge shifts to lower wavenumbers. The position of the absorption edge for 2LT aerogel (not shown) at around $34,000\text{ cm}^{-1}$ is almost the same as that for TS-1. We propose that in this sample most of the titanium is atomically mixed in the silica matrix. The shift towards lower wavenumbers in the spectra of 5, 10, and 20LT aerogels compared to TS-1 indicates that, besides atomically mixed titanium, some nanodomains of titania must also exist in these samples. The UV absorption threshold is a function of titania cluster size for diame-

ters less than 10 nm (quantum size effect, (40)). As the size of the titania domains grows with increasing Ti content in the mixed oxides, the observed absorption edge is located closer and closer to that characteristic of bulk anatase. This conclusion is supported by the quantitative analysis of the FTIR spectra reported in part I (22) of this series. The Si–O–Ti connectivity $D_{(\text{Si-O-Ti})}$ defined as the ratio of the deconvoluted peak areas of the $\nu(\text{Ti-O-Si})$ vibration at ca. 940 cm^{-1} and $\nu(\text{Si-O-Si})$ vibration at ca. 1210 cm^{-1} is the highest and about the same for TS-1 and 2LT aerogel, and decreases monotonically with increasing Ti content in the LT aerogel series (Table 2 in part I (22)).

We found that dehydration of the samples at 473 K for 5 h shifted the absorption edge to higher wavenumbers by about 1500 cm^{-1} in all LT aerogel samples but did not change their position relative to anatase. An even more pronounced shift (ca. 4000 cm^{-1}) is observed for TS-1 when applying the same drying procedure. It has been proposed that water adsorption disturbs the regular tetrahedral structure surrounding titanium in the silica-rich sample (19, 37, 41). Note that in Fig. 7 the spectra recorded under ambient conditions are shown.

The effect of H_2O_2 treatment of the three typical titania–silica samples is shown in Fig. 8. The interaction of the Ti species with peroxide results in an increase of the absorption in a broad range up to $32,000\text{ cm}^{-1}$ for the LT aerogels and xerogels, but not for the HT aerogels (Fig. 8). These spectral changes are supported by the observation that LT aerogels and xerogels turn strong yellow upon impregnation with peroxide, whereas the HT aerogels preserve their beige colour. The H_2O_2 addition followed by its thermal treatment and dehydration represents a cyclic treatment: heating the samples at 333 K for a period of 2 h restores the original spectra. Earlier studies made on titanium silicalite (38, 41) revealed a similar effect in the charge transfer characteristics upon H_2O_2 treatment, which is explained by the formation of surface peroxides.

The interpretation of the FTIR and UV–vis spectra of sol-gel titania–silica catalysts is in agreement with the XRD analysis reported in part I (22). No crystalline titania could be detected in xerogels and LT aerogels, but 5HT and 10HT aerogels contained anatase particles of ca. 8 nm mean size.

Influence of Reaction Parameters

The role of some important reaction variables is discussed shortly below. An increase in reaction temperature accelerates the epoxidation with a minor decrease in selectivity. The rate acceleration effect using LT aerogels at 333 and 363 K can be seen from comparison of Figs. 2 and 5. Most of the epoxidation reactions were performed at 333 K, at which temperature both rate and selectivity are high. The selectivity S_{peroxide} decreased slightly from

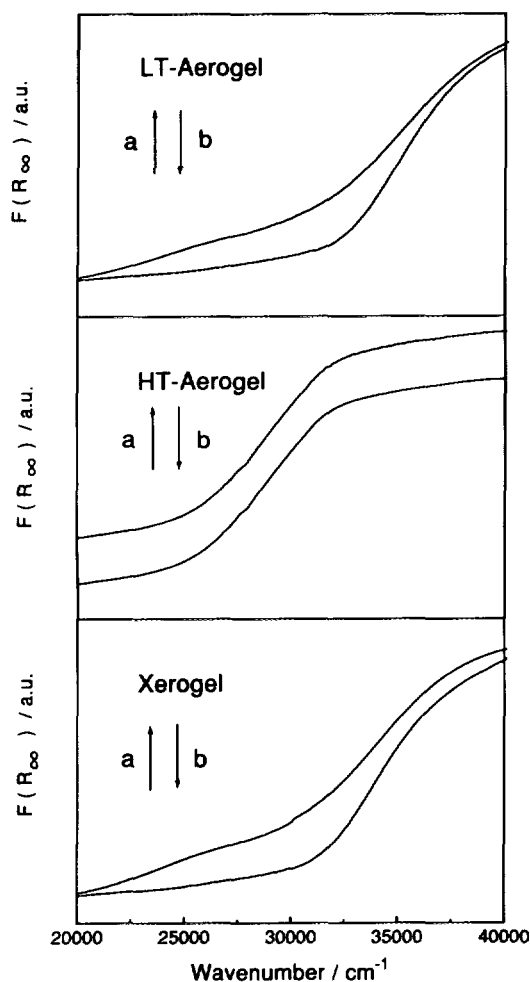


FIG. 8. Diffuse reflectance spectra of 10LT aerogel (top), 10HT aerogel (middle), and 10X xerogel (bottom) after H_2O_2 adsorption (a) and after subsequent heating at 333 K (b).

93 to 91% when the temperature was raised from 333 to 363 K, but the epoxidation remained a quantitative reaction based on the olefin.

It was proved in two different ways that the sol-gel catalysts really act as heterogeneous catalysts. Their good catalytic performance is not due to some Ti complex formation and homogeneous catalysis. After reaction the catalysts were filtered off and analyzed. ICP-AES analysis and IR characterization (intensity of the band at about 950 cm^{-1}) showed no detectable leaching of titanium from the catalysts during epoxidation. Besides, the reactions stopped after removal of the catalyst by filtration.

Slow dosing of CHP did not improve the selectivity, compared to the reactions when CHP was added at the beginning. Similarly, the use of *t*-butylhydroperoxide instead of CHP did not result in considerable changes in the reaction characteristics. However, all sol-gel titania-silica samples were inactive when using H_2O_2 as oxi-

dant owing to severe inhibition of the catalyst by water (2) and to leaching of Ti from the solid.

When using CHP as oxidant, the typical coproduct is 2-phenyl-2-propanol. The deliberate addition of 2-phenyl-2-propanol (peroxide/alcohol molar ratio = 1/1) to the reaction mixture lowered the reaction rate by only ca. 10%, without any influence on selectivity. The suppression of activity is likely due to the general effect of polar solvents, which compete for the active coordination sites and suppress the epoxidation reaction (2, 27).

Peroxide Decomposition

Peroxide decomposition is the most important side reaction during olefin epoxidation. Figure 9 shows the CHP conversion in cumene over various catalysts. In the absence of any catalyst less than 5% of the peroxide was decomposed after 16 h (not shown in Fig. 9). A similar rate was observed in the presence of silica. The 10HT aerogel shows only a slightly enhanced activity for peroxide decomposition compared to silica, significantly lower than the rate observed for the 10LT aerogel. The highest activity for CHP decomposition was observed on titania which, however, was suppressed considerably when cyclohexene was added (molar ratio olefin/peroxide = 1/1) to the reaction mixture. It is clear from the selectivities shown in Table 1 that when both CHP and olefin are present the rate of olefin epoxidation compared to that of CHP decomposition was the highest on LT aerogels.

Oxidation of Various Olefins

The catalytic performance of the raw 20LT aerogel in the epoxidation of some alkenes is illustrated in Table 3.

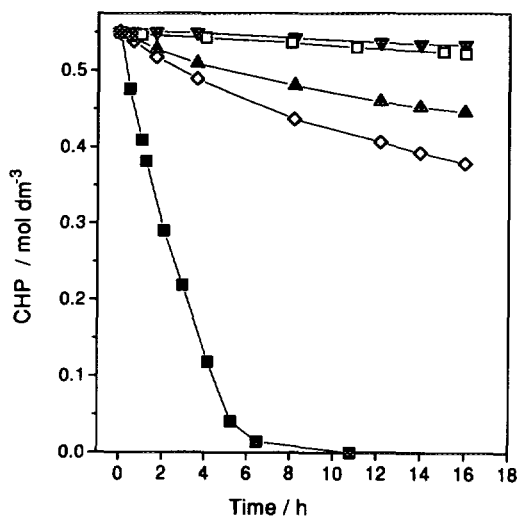


FIG. 9. CHP decomposition over various oxides: SiO_2 (Aerosil 200) (\blacktriangledown), 10HT calcined at 873 K (\square), 10LT calcined at 873 K (\blacktriangle), TiO_2 (P25) with cyclohexene added (\diamond), and TiO_2 (P25) (\blacksquare); (CHP: 0.55 M; catalyst: 0.2 g; 333 K).

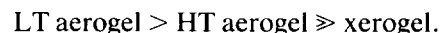
Bulky molecules, which are not oxidized by TS-1, are readily epoxidized by the sol-gel catalyst. Selectivities related to both the peroxide and the olefin are good or excellent. The high selectivity related to the olefin is of great importance for the epoxidation of fine chemicals, as olefins can be very precious reactants. The reaction rate strongly depends on the structure of the olefin. It seems that the epoxidation of cyclic olefins is much faster than that of acyclic alkenes. Further investigation is planned applying even bulkier reactants.

DISCUSSION

Systematic development of titania-silica mixed oxides (22) prepared by an alkoxide-sol-gel route resulted in very active and selective catalysts for the epoxidation of olefins with alkylhydroperoxides. The crucial parameters of catalyst development were the drying method and the Ti content. Interestingly, the catalytic performance of aerogels or xerogels could not be improved by calcination at temperatures between 473 and 1073 K. Apparently, the presence of organic residues from catalyst preparation (up to 10 wt% carbon content) slightly favours the epoxidation reaction.

The aerogels dried by semicontinuous extraction with supercritical CO₂ at low temperature (313 K, LT aerogel) show high epoxidation activity and high selectivity to both

the olefin (up to 100%) and the peroxide. Cyclohexene was chosen as a model reactant and CHP was used as oxidant during the development procedure, but the catalysts are also active with other alkylhydroperoxides (e.g., *t*-butyl hydroperoxide) and able to selectively oxidize bulkier cyclic olefins, such as cyclododecene. When comparing the aerogels and xerogels prepared in the same way but using different drying procedures, the following general order can be written for their activity:



In the following subsection we shall discuss the interesting question, what are the characteristics of LT aerogels which make them superior to other titania-silica catalysts in the epoxidation of bulky cyclic olefins?


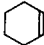
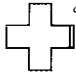
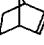
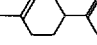
Characteristics of LT Titania-Silica Aerogels

In part I (22) all LT aerogels were found to be X-ray amorphous even after calcination at 1073 K. Their BET surface areas varied between 410 and 683 m² g⁻¹, increasing with the Ti content and having maxima after calcination at 683 K. The high surface area seems to be an important requirement for high oxidation activity.

Based on nitrogen physisorption experiments (22), the mean cylindrical pore diameter ($\langle d_p \rangle$) was moderate for 2LT aerogels: 2–4 nm, depending on the calcination temperature. At higher Ti content microporosity diminished and the 5LT, 10LT, and 20LT samples were mesoporous with $\langle d_p \rangle$ of 8–14 nm, varying with the Ti content and calcination temperature. The pore size maxima were considerably higher, between 40 and 70 nm, for all LT aerogels. The estimated size of cumene hydroperoxide (oxidant) in its minimum energy conformation is 0.55 × 0.63 × 0.93 nm. Cyclohexene (reactant) and cumene (solvent) are somewhat smaller, but still comparable to the diameter of a fraction of the pores in 2LT aerogel. Accordingly, a moderate transport limitation can be expected in the epoxidation reaction with the 2LT aerogel. This diffusion problem should be absent in aerogels of higher Ti content in which the active sites in the pores are easily accessible even to the bulkiest reactant investigated (cyclododecene: 0.48 × 0.83 × 0.90 nm).

Despite the several physicochemical methods applied for the characterization of LT aerogels, we do not have unambiguous evidence concerning the nature of active sites. We propose that there are two types of active sites present in LT aerogels. The more active species in olefin epoxidation is the highly dispersed, probably isolated titanium surrounded by –O–Si–O–Si–O– structural elements in all directions (8). The other, less active species is Ti connected to –O–Si–O– species as well as to other Ti atoms via oxygen (–O–Ti–O–). We can visualize these Ti

TABLE 3
Conversions and Selectivities in the Epoxidation of Various Olefins^a

| Olefin | Time for 50% CHP conversion (min) | Time for 95% CHP conversion (min) | Selectivity (%) ^b | |
|---|---|---|---------------------------------|----------------------------|
| | | | <i>S</i> _{peroxide} | <i>S</i> _{olefin} |
|  | 80 | — | 85 ^c | 95 |
|  | 3.4 | 15 | 91 | 100 |
|  | 10 | 120 | 89 | 95 |
|  | 7 | 59 | 92 | 97 ^e |
|  | 7 | 30 | 79 ^f | 87 ^f |

^a Reaction conditions: 363 K, 0.1 g 20LT aerogel (raw), 60 mmol olefin, 13.4 mmol CHP.

^b At 95% CHP conversion.

^c At 50% CHP conversion.

^d Mixture of *cis* and *trans*.

^e Exo- and endo-epoxides.

^f Selectivity to 4-isopropenyl-1-methyl-1-cyclohexene-1,2-epoxide.

atoms as located at the "border" of titania nanodomains. These small amorphous titania agglomerates are also well-dispersed in (on) the silica matrix and their size varies from a few atoms up to a few nanometers.

In part I of this work (22) the deconvoluted peak area of the $\nu(\text{Ti-O-Si})$ vibration at ca. 940 cm^{-1} was related to that of the $\nu(\text{Si-O-Si})$ vibration at ca. 1210 cm^{-1} and normalized to the Ti content. This ratio denoted $D_{(\text{Si-O-Ti})}$ was highest for the 2LT aerogel (about the same as for TS-1) and decreased with increasing Ti content. This result, together with the almost identical position of the UV-vis absorption edge of 2LT aerogel and TS-1, suggests that in 2LT catalyst Ti is highly (probably atomically) dispersed in silica and there is not detectable amount of titania domains. Despite the very similar specific intensity of the Ti-O-Si vibration in TS-1 and 2LT, the specific rate of cyclohexene epoxidation with an alkylhydroperoxide was higher (by a factor of ca. 250) with 2LT. The difference is likely due to the larger pore diameter of the aerogel and thus better accessibility of active sites.

Both the IR band at ca. 950 cm^{-1} and the epoxidation activity developed monotonically but not linearly when the overall titania content was increased from 2 to 20 wt% (Fig. 4). We assume that this is due the formation of titania nanodomains, which is indicated by the FTIR studies of part I (22) and independently by the DRS investigations. The higher the overall Ti content, the higher the shift of the absorption edge was observed, showing an increasing proportion of Ti located in titania nanodomains.

Further evidence for this segregation effect occurring at higher Ti content emerges from the Ti dispersions reflected by the $D_{(\text{Si-O-Ti})}$ values determined in part I (22). They indicate that Ti dispersion decreases with increasing Ti content. Accordingly, the highest specific activity (expressed as turnover frequency TOF, mol converted reactant per mol Ti per unit time) can be expected for the lowest Ti content. It is shown in Fig. 10 that this expectation is not fulfilled: the 2LT aerogel exhibits considerably lower initial rate (TOF) in cyclohexene epoxidation than 5LT or 10LT. The likely explanation is the above-mentioned diffusion limitation presumed for this sample. For comparison, the mean cylindrical pore diameters ($\langle d_p \rangle$) of LT aerogels (22) used in the oxidation reaction are also plotted in Fig. 10. We can conclude that the advantageous morphological changes compensate the lower activity of the increasing amount of dispersed titania nanodomains in aerogels containing 5 and 10 wt% TiO_2 .

Unlike in oxidations performed with TS-1, where extra framework Ti (above ca. 3 wt%) or titania is active in peroxide decomposition but inactive in olefin epoxidation (30), our catalytic experiments proved that the amorphous titania LT aerogel has some moderate activity and higher than 60% selectivity in the epoxidation of cyclohexene with CHP. It is not surprising that the activity and selectiv-

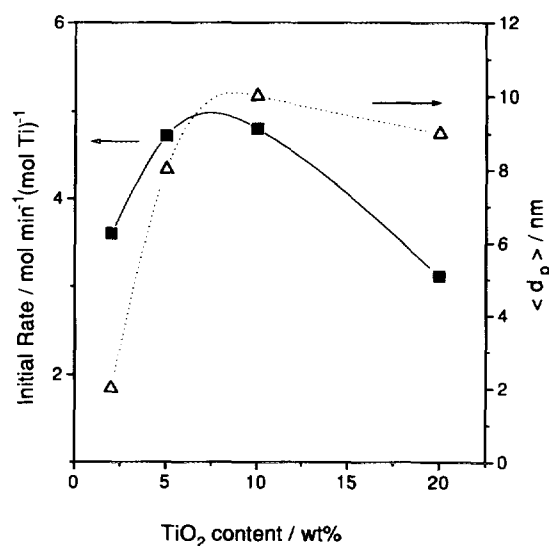


FIG. 10. Initial rate of cyclohexene epoxidation (■) and mean cylindrical pore diameter (△) (from Ref. (22)) of LT aerogels after calcination at 673 K.

ity of small titania domains are even higher and approach those of isolated Ti-O-Si species when they are well-dispersed in the silica matrix. This is a feasible explanation for the monotonic (but nonlinear) increase of epoxidation activity of LT aerogels with increasing overall titania content up to 20 wt%.

Influence of Drying Methods

Whereas titania-silica LT aerogels are active and selective epoxidation catalysts in liquid phase, xerogels, prepared in the same way but conventionally dried at 313–373 K, show no activity for epoxidation. No major differences are found using FTIR, UV-vis, and XRD characterization. Both amorphous solids have a comparable high degree of titanium dispersed in the silica matrix. The spectral changes induced by a treatment with H_2O_2 show the same characteristics for both types of catalysts: there are reactive species on the catalyst surface. However, a major difference exists in the morphology. The LT aerogels exhibit a pronounced mesoporosity, whereas the xerogels are predominantly microporous, with $\langle d_p \rangle$ considerably lower than 2 nm (22). The inactivity of the xerogels is therefore supposed to be a consequence of the limited accessibility of active sites for the bulky oxidant CHP. The diffusion of the much smaller H_2O_2 is not hindered and the surface active sites form peroxy complexes with it, as proved by spectroscopic analysis. The development of a micropore structure (by collapsing of the network during conventional drying due to capillary forces) can be avoided only by the supercritical drying procedure applied in the preparation of LT aerogels.

HT aerogels, dried under supercritical conditions at 533 K (22), show some activity in cyclohexene epoxidation, but this activity is low compared to LT aerogels. Similarly, selectivities related to both peroxide and olefin are distinctly lower for HT aerogels. The morphology of HT aerogels cannot explain the low activity: the meso- to macroporous materials have $\langle d_p \rangle$ of 19–24 nm, which excludes any diffusion limitation. Spectroscopic investigations disclosed major differences between LT and HT aerogels. The significantly lower intensity of the band at about 950 cm^{-1} for HT aerogels (Table 1 and part I (22)) indicates that these solids have a low proportion of isolated titanium in the silica matrix. The practically undetectable spectral change expected after a treatment with H_2O_2 is a further sign of the minor amount of reactive isolated titanium species. XRD analysis (22) indicated the presence of anatase particles with ca. 8 nm average crystallite size. The high-temperature drying procedure induces a considerable segregation and agglomeration of titania and silica, which destroys the advantageous structure developed during the sol-gel procedure and results in a dominance of titanium located in hardly active anatase particles. This behaviour has been indicated by XRD as well as vibrational spectroscopy (22) and has been further confirmed by DRS and the catalytic studies.

Comparison of LT Titania–Silica Aerogels to Other Types of Titania–Silica Catalysts

Among all the sol-gel titania–silica catalysts studied, the 20LT aerogels possess the highest activity related to the amount of catalyst. These catalysts were shown to be superior to titania-on-silica in the epoxidation of cyclohexene with CHP (Table 2). The performance of TS-1 in this reaction is not surprising. It is well-known (11) that the activity of TS-1 is excellent for lower olefins but poor in the epoxidation of cyclohexene and other bulky reactants due to steric limitation in the pores of ca. 0.55 nm.

Recently some papers have been published in which the authors proposed to solve the steric limitation in TS-1 by synthesizing large- and ultralarge-pore Ti-zeolites (12–14). Ti-Beta, a typical large-pore zeolite, has a pore diameter of about 0.65 nm. Simple aliphatic olefins, such as 1-octene, are readily oxidized by this zeolite (42–44), but the reaction is slow when norbornene, α -terpineol, or cyclododecene is used as a model compound (45, 46). We compared Ti-Beta with our 20LT catalyst in the epoxidation of cyclododecene (data for 20LT are in brackets): 33 (60) mmol olefin was oxidized over 200 (100) mg catalyst with 8.4 (13.4) mmol H_2O_2 (CHP) at 353 (363) K; after 60 min the peroxide conversion was 3.8 (77.1) %. There is a striking difference in favour of the sol-gel catalyst. The reaction conditions (temperature, reaction time) are similar, except that the catalyst/olefin ratio is

almost four times smaller in the case of 20LT. Moreover, the selectivity to epoxide was only 88% with the zeolite even at this low conversion due to glycol formation, while 20LT provided 95% selectivity up to 95% CHP conversion.

Ti-MCM-41, an ultralarge-pore Ti-zeolite with pores of about 2–3 nm (13, 46) is a better candidate for oxidizing bulky reactants. It has been reported (46) that its activity is about 3 times higher than that of Ti-Beta in the epoxidation of norbornene. 26.4% epoxide and 3.1% alcohol were obtained with Ti-MCM-41 and *t*-butyl hydroperoxide in 5 h. The calculated average reaction rate related to the amount of catalyst is higher by more than two orders of magnitude for 20LT (Table 3) compared to Ti-MCM-41. However, a direct comparison of the two catalysts is not possible due to the lower temperature and the unusually high catalyst/olefin (0.94/1) and peroxide/olefin weight ratios applied for the zeolite catalyzed epoxidation.

CONCLUSIONS

Amorphous sol-gel titania–silica LT aerogels are novel catalysts, very active and selective catalysts for the epoxidation of bulky olefins in the liquid phase. The combined physicochemical and catalytic study of various titania–silica aerogels and xogels indicates that high epoxidation activity can be expected only when titanium is well-dispersed in the silica matrix and the solid possess a mesoporous structure. The catalytic activity of titania–silica aerogels in the epoxidation of olefins by CHP is related to the presence of Ti–O–Si structural parts and to a lower extent to unstructured titanium-oxo domains.

ACKNOWLEDGMENTS

The authors are grateful to Reiner Glöckler and Professor Jens Weitkamp for kindly supplying the TS-1 sample. Thanks are also due Helmut Schneider for his help in spectroscopic analysis. Financial support of this work by F. Hoffmann-La Roche AG, Switzerland, and the Kommission zur Förderung der wissenschaftlichen Forschung is gratefully acknowledged.

REFERENCES

1. Jørgensen, K. A., *Chem. Rev.* **89**, 431 (1989).
2. Sheldon, R. A., *J. Mol. Catal.* **7**, 107 (1980).
3. U.K. Patent 1,249,079 (1971).
4. U.S. Patent 3,923,843 (1975).
5. Notari, B., *Stud. Surf. Sci. Catal.* **37**, 413 (1988).
6. U.S. Patent 4,410,501 (1983).
7. Reddy, J. S., Kumar, R., and Ratnasamy, P., *Appl. Catal.* **L1**, 58 (1990).
8. Notari, B., *Catal. Today* **18**, 163 (1993).
9. Clerici, M. G., Bellussi, G., and Romano, U., *J. Catal.* **129**, 159 (1991).
10. Hutchings, G. J., and Lee, D. F., *J. Chem. Soc. Chem. Commun.*, 1095 (1994).
11. Clerici, M. G., and Ingallina, P., *J. Catal.* **140**, 71 (1993).

12. Camblor, M. A., Corma, A., Martínez, A., and Pérez-Pariente, J., *J. Chem. Soc. Chem. Commun.*, 589 (1992).
13. Corma, A., Navarro, M. T., and Pérez-Pariente, J., *J. Chem. Soc. Chem. Commun.*, 147 (1994).
14. Corma, A., Camblor, M. A., Esteve, P., Martínez, A., and Pérez-Pariente, J., *J. Catal.* **145**, 151 (1994).
15. Huybrechts, D. R. C., Buskens, Ph., and Jacobs, P. A., *Stud. Surf. Sci. Catal.* **72**, 21 (1992).
16. Hayashi, T., Yamada, T., and Saito, H., *J. Mater. Sci.* **18**, 3137 (1983).
17. Schraml-Marth, M., Walther, K. L., Wokaun, A., Handy, B. E., and Baiker, A., *J. Non-Cryst. Solids* **143**, 93 (1992).
18. U.S. Patent 5,162,283 (1992).
19. Liu, Z., and Davis, R. J., *J. Phys. Chem.* **98**, 1253 (1994).
20. Neumann, R., Chava, M., and Levin, M., *J. Chem. Soc. Chem. Commun.*, 1685 (1993).
21. Khouw, C. B., Li, H. X., Dartt, C. B., and Davis, M. E., in "Catalytic Selective Oxidations" (S. T. Oyama and J. W. Hightower, Eds.), p. 273, ACS Symp. Ser., Vol. 523. Am. Chem. Soc., Washington, DC, 1993.
22. Dutoit, D. C. M., Schneider, M., and Baiker, A., *J. Catal.* **153**, 165-176 (1995).
23. Dutoit, D. C. M., Schneider, M., and Baiker, A., submitted for publication.
24. Martens, J. A., Buskens, Ph., Jacobs, P. A., van der Pol, A., van Hooff, J. H. C., Ferrini, C., Kouwenhoven, H. W., Kooyman, P. J., and van Bekkum, H., *Appl. Catal. A* **99**, 71-84 (1993).
25. Kubelka, P., and Munk, F., *Z. Tech. Phys.* **12**, 593 (1931).
26. Mair, R. D., and Graupner, J., *Anal. Chem.* **36**, 194 (1964).
27. Sheldon, R. A., and Kochi, J. K., "Metal-Catalysed Oxidations of Organic Compounds." Academic Press, San Diego, 1981.
28. Schuck, G., Dietrich, W., and Fricke, J., in "Aerogels, Proceedings of the 1st International Symposium on Aerogels, ISA1" (J. Fricke, Ed.), p. 142. Springer Proceedings in Physics, Vol. 6, Springer, Berlin, 1986.
29. Srinivasan, S., Datye, A. K., Hampden-Smith, M., Wachs, I. E., Deo, G., Jehng, J. M., Turek, A. M., and Peden, C. H. F., *J. Catal.* **131**, 260 (1991).
30. Huybrechts, D. R. C., Buskens, Ph., and Jacobs, P. A., *J. Mol. Catal.* **71**, 129 (1992).
31. Boccuti, M. R., Rao, K. M., Zecchina, A., Leofanti, G., and Petrini, G., *Stud. Surf. Sci. Catal.* **48**, 133 (1989).
32. Perego, G., Bellussi, G., Corno, C., Taramasso, M., Buonomo, F., and Esposito, A., *Stud. Surf. Sci. Catal.* **28**, 129 (1986).
33. Trong On, D., Bonneviot, L., Bittar, A., Sayari, A., and Kaliaguine, S., *J. Mol. Catal.* **74**, 233 (1992).
34. Bellussi, G., and Fattore, V., *Stud. Surf. Sci. Catal.* **69**, 79 (1991).
35. Jacobs, P. A., in "Tagungsbericht, Vol. 9204" (M. Baerns and J. Weitkamp, Eds.), p. 171. DGMK, Hamburg, 1992.
36. Bräutigam, U., Meyer, K., and Bürger, H., in "EUROGEL '91" (S. Vilminot, R. Nass and H. Schmidt, Eds.), p. 335, Elsevier, Amsterdam, 1992.
37. Beghi, M., Chiurlo, P., Costa, L., Palladino, M., and Pirini, M. F., *J. Non-Cryst. Solids* **145**, 175 (1992).
38. Huybrechts, D. R. C., Vaesen, I., Li, H. X., and Jacobs, P. A., *Catal. Lett.* **8**, 237 (1991).
39. Zecchina, A., Spoto, G., Bordiga, S., Padovan, M., Leofanti, G., and Petrini, G., *Stud. Surf. Sci. Catal.* **69**, 671 (1991).
40. Fernandez, A., Leyrer, J., González-Elipé, A. R., Munuera, G., and Knözinger, H., *J. Catal.* **112**, 489 (1988).
41. Geobaldo, F., Bordiga, S., Zecchina, A., Giamello, E., Leofanti G., and Petrini, G., *Catal. Lett.* **16**, 109 (1992).
42. Sato, T., Dakka, J., and Sheldon, R. A., *J. Chem. Soc. Chem. Commun.*, 1887 (1994).
43. Sato, T., Dakka, J., and Sheldon, R. A., *Stud. Surf. Sci. Catal.* **84**, 1853 (1994).
44. Rigutto, M. S., de Ruiter, R., Niederer, J. P. M., and van Bekkum, H., *Stud. Surf. Sci. Catal.* **84**, 2245 (1994).
45. Camblor, M. A., Corma, A., Martínez, A., Pérez-Pariente, J., and Primo, J., *Stud. Surf. Sci. Catal.* **78**, 393 (1994).
46. Corma, A., Navarro, M. T., Pérez-Pariente, J., and Sánchez, F., *Stud. Surf. Sci. Catal.* **84**, 69 (1994).